1

Introduction to Early Main Group Organometallic Chemistry and Catalysis

Sjoerd Harder

University Erlangen-Nürnberg, Inorganic and Organometallic Chemistry, Egerlandstrasse 1, 91058 Erlangen, Germany

1.1 Introduction

Although organometallic complexes of the early main groups are well known for their very high reactivity and challenging isolation, they are among the first studied during the pioneering beginnings of the field. Their high nucleophilicity and Brønsted basicity have made them to what they are today: strong polar reagents that are indispensible in modern organic synthesis. It is exactly this high reactivity that has made them potent catalysts for organic transformations that are generally catalyzed by transition metal complexes. Despite their lack of partially filled d-orbitals and their inability to switch reversibly between oxidation states, the scope of their application in catalysis is astounding. As the early main group metal catalysis only started to become popular since the beginning of this century, it is still a young field with ample opportunities for further development. This introductory chapter is specifically written for new graduate students in the field. It gives a very compact overview of the history of early main group organometallic chemistry, synthetic methods, bonding and structures, analytical methods, solution dynamics, and some preliminary low-valent chemistry. This forms the basis for understanding their use in catalysis for which the basic steps are described in the second part of this chapter. For further in-depth information, the reader is referred to the individual chapters in this book.

1.2 s-Block Organometallics

1.2.1 Short History

The organometallic chemistry of the highly electropositive early main group metals could not have started without the isolation of these elements in the metallic state. Being only available in nature in the form of their salts, the invention of electricity and electrolysis in the beginning of 1800s has been the key to their isolation. The legendary Humphry Davy (1778–1829) can claim the

Early Main Group Metal Catalysis: Concepts and Reactions,
First Edition. Edited by Sjoerd Harder.

discovery of at least seven s-block metals: the alkali metals Li, Na, and K and the alkaline earth (Ae) metals Mg, Ca, Sr, and Ba.

Most organometallic classes start with Frankland's well-known synthesis of Et_2Zn in 1847 [1] by reaction of Zn and EtI, which was originally an attempt to isolate the Et radical. It is, however, less known that before this experiment, Frankland tried to isolate the Et radical by mixing K and EtI, a reaction that was found to be very violent producing a variety of gaseous products [2]. Wanklyn reacted Frankland's Et_2Zn with Na and isolated the zincate $Na^+ZnEt_3^-$, which, based on its very high reactivity, was described as a solution of EtNa in Et_2Zn. Although not metal pure, this is likely the first preparation of an alkylsodium compound. Numerous early organometallic pioneers attempted to prepare organosodium complexes directly by reaction of the metal with R–X (R = alkyl or aryl; X = Cl, Br, and I) but never isolated the organosodium products that were found to be fleeting intermediates to Wurtz (or Wurtz–Fittig) R–R coupling products.

Switching to the less reactive metal Li, Wilhelm Schlenk was the first to isolate group 1 alkylmetal complexes in a pure form. Reduction of Me_2Hg with Li metal gives metallic mercury and MeLi as a white powder. Schlenk describes the pyrophoric nature of this powder in beautiful words, clearly demonstrating his fascination for these compounds [3]. Although Schlenk is not just the "man behind the flask" [4] but certainly also a major pioneer in organometallic chemistry of the alkali metals, it was Karl Ziegler who developed the simple mercury-free route to organolithium reagents [5], which is the method of choice even today for the synthesis of *n*BuLi: $n\text{BuCl} + 2\text{Li}^0 \rightarrow n\text{BuLi} + \text{LiCl}$. Because alkyllithium reagents are less reactive than Na or K reagents, Wurtz coupling is limited. Also, their much higher solubility in apolar organic solvents added to their successful isolation. The latter strong alkyllithium base is not only the starting point for modern organolithium chemistry but also for the development of superbases based on the heavier alkali metals.

Grignard developed organometallic chemistry of group 2 metals and reported in 1900 a similar protocol to prepare organomagnesium reagents: $\text{R–X} + \text{Mg} \rightarrow \text{RMgX}$ [6]. Foreseeing a great future for these potent reagents, Grignard was awarded the Nobel Prize for this milestone discovery already in 1912. Similar to group 1 metals, the development of the organometallic chemistry of the heavier group 2 metals was found to be more challenging. Beckmann mentioned already in 1905 the first synthetic routes to arylcalcium halides [7] but Gilman had problems reproducing these results [8]. Development of the organometallic chemistry of the heavier Ae metals turned out to be substantially more difficult than simply reproducing the Grignard method with Ca instead of Mg.

1.2.2 Synthesis of Group 1 Organometallics

A short overview of synthetic methods to pure organoalkali metal compounds is shown in Scheme 1.1 (for comprehensive reviews, see [9, 10]). The synthesis of *n*BuLi directly from its metal and *n*BuCl stands central to the further development of lithium chemistry. The highly Brønsted basic $n\text{Bu}^-$ anion (approximate pK_a of CH_3 in butane ≈ 50 [11, 12]) is able to deprotonate a large variety of

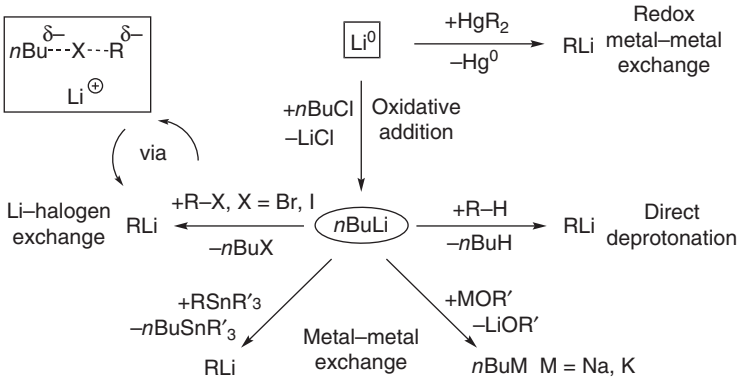

Scheme 1.1 Overview of common synthetic routes to organolithium compounds.

organic substrates with pK_a's up to 45 (e.g. benzene) provided the *n*BuLi reagent is sufficiently activated by polar cosolvents (see Section 1.2.3). For problematic deprotonation reactions, the even stronger base *t*BuLi is routinely used (approximate pK_a of CH in 2-methylpropane ≈ 52 [11, 12]). Direct substrate deprotonation with alkyllithium reagents has the great advantage that the alkane side product is volatile and easily removed. Its disadvantage is that the selectivity of product formation is controlled by the substrate's acidity. In some cases, however, complex formation between substrate and alkyllithium reagent controls the selectivity of deprotonation by the complex-induced-proximity-effect (CIPE) [13] influencing the kinetics and thermodynamics of product formation. The well-known Li–halogen exchange route allows exact regiocontrol of the deprotonation reaction. In polar solvents, this conversion is even extremely fast at −80 °C. The mechanism proceeds through a hypervalent C–X–*n*Bu intermediate because only heavier halogens (X = Br and I) can be used. Also, for these reactions, it holds that the product carbanion should be more stable than the $n\text{Bu}^-$ anion. For the identity exchange reaction, $C_6F_5I + C_6F_5Li$, the hypervalent intermediate $[Li^+\cdot(TMEDA)_2][C_6F_5\text{–}I\text{–}C_6F_5^-]$, has been structurally characterized [14]. The Li–halogen exchange is limited to lithiations of sp^2 C atoms because sp^3 C–X groups are prone to S_N2 substitution. The product isolation is sometimes complicated by the subsequent S_N2 reaction of the organolithium product with the side product *n*BuX. Another method for selective lithiation is Li–Sn exchange, which proceeds through a hypervalent intermediate with retention at Sn and C [15].

Reagents based on the heavier alkali metals Na and K cannot be prepared by the direct reaction of an organohalide with the metal because of Wurtz coupling. A simple route for the preparation of the highly reactive superbases *n*BuNa and *n*BuK consists of mixing *n*BuLi with the higher metal alkoxide *t*BuOM (M = Na and K) [16]. This metal exchange reaction is based on the hard-soft-acid-base (HSAB) principle: the smaller (harder) Li^+ prefers to interact with the smaller (harder) O^- of the alkoxide, whereas the larger (softer) Na^+ and K^+ prefer interaction with the larger (softer) C^- in the carbanion. As the early pioneers in this area, Lochmann and Schlosser [17], disputed this invention, these reagents

are known as Lochmann or Schlosser bases. However, their roots go back much further when Morton and Chester reported the highly basic properties of RNa/LiOR mixtures [18]. The more correct naming of these mixtures as "superbases" reveals that these reagents are indeed very powerful deprotonation reagents. Their very high reactivity originates from their longer (and weaker) bonds, which facilitate the kinetics of the bond-breaking and bond-making processes. Use of heterobimetallic reagents consisting of an alkalimetal and Mg, Zn, or Al brought the synthetic utility of alkali metal reagents even to a higher level [19]. Template-controlled interaction with the substrate results in deprotonation at unusually mild conditions or with unusual regioselectivities and often polydeprotonations can be achieved.

1.2.3 Synthesis of Group 2 Organometallics

With few exceptions, preparative methods for the organometallic complexes of group 2 were, for a long time, limited to Mg Grignard reagents [20]. Although it is suggested that health risks concerned with Be chemistry can be mastered [21], there are still not many practitioners in this area. The interest in the organometallic chemistry of the heavier metals Ca, Sr, and Ba, however, is rapidly growing because of their application in MOCVD (metal-organic chemical vapor deposition) [22] and homogeneous catalysis [23]. As mentioned previously, organocalcium complexes cannot be prepared by simply replacing Mg for Ca in the Grignard synthesis (Scheme 1.2). Similar to organosodium or potassium compounds, the much more potent "Ca Grignards" may also react with the organohalide to Wurtz-type products. Because nucleophilic aromatic substitution is more difficult, arylcalcium Grignard reagents (ArCaI) could be isolated but only under controlled conditions, which involve low temperature and special activation methods for the Ca metal used [24]. For the magnesium Grignard, ethereal solvents must be used; however, ArCaI is much more reactive

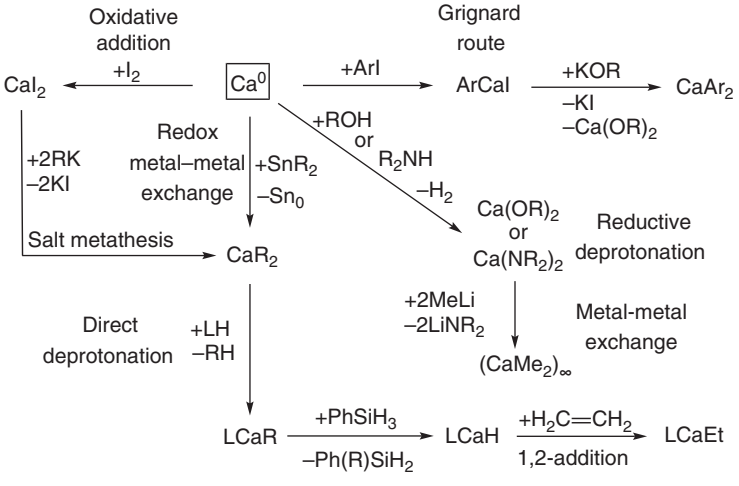

Scheme 1.2 Overview of common synthetic routes to organocalcium compounds.

that it is easily decomposed by ether deprotonation. The temperature during the synthesis is generally maintained below −40 °C, but the Ca Grignard is more stable as thought initially: *para*-tolylcalcium iodide in tetrahydrofuran (THF) has a half-life time of eight days. The arylcalcium complex is more stable in tetrahydropyran (THP) in which the half-life time is increased to 17 days.

Similar to the original magnesium Grignard, Ca Grignard reagents are also susceptible to the Schlenk equilibrium [25]: $2ArCaI \rightleftharpoons Ar_2Ca + CaI_2$. The synthesis of homoleptic organomagnesium reagents can be simply achieved by addition of dioxane to the RMgX solution, which results in immediate precipitation of $MgX_2 \cdot$(dioxane), leaving R_2Mg in solution. Although this procedure does not work for heavier Ca Grignards, Westerhausen and coworkers reported an elegant procedure that involves addition of KO*t*Bu [26]. This results in conversion of ArCaI into insoluble KI and ArCaO*t*Bu, which after ligand exchange leads to precipitation of $[Ca(OtBu)_2]_\infty$, leaving Ar_2Ca in the solution.

The very high reactivity of arylcalcium reagents may be exploited in specialty applications but inherently also makes these complexes highly sensitive toward decomposition by air and/or solvents. Therefore, the most popular Ca reagents are to some extent stabilized by bulky and/or electron-withdrawing groups. Westerhausen and coworkers reported the syntheses of the whole range of bis-trimethylsilylamide complexes $Ae[N(SiMe_3)_2]_2$ (Mg, Ca, Sr, and Ba) by reduction of the Sn(II) complex $Sn[N(SiMe_3)_2]_2$ with Ae^0 [27]. These homoleptic amide complexes, abbreviated by AeN''_2, are likely the most widely used starting reagents in heavier Ae metal chemistry. They can also be prepared by salt metathesis, reacting AeI_2 with 2 equiv of KN″ [28]. Generally, metal iodide salts are chosen as the precursor on account of their better solubility while potassium reagents are favored because of complete insolubility of KI in ethereal solvents. A major disadvantage of the salt metathesis route is the possible formation of "ate" complexes, $[K^+][AeN''^-_3]$, a side product that cannot always be detected by nuclear magnetic resonance (NMR) even in considerable quantities [29]. The other disadvantage of the salt metathesis route is the fact that ethereal solvents have to be used and therefore complexes are always isolated in the form of their etherates. The Sn route can be performed in aromatic solvents giving solvent-free, metal-pure, products AeN''_2, but sometimes, the separation of the very fine Sn particles can be problematic.

The salt metathesis route is probably the most popular pathway to homoleptic complexes and also the procedure of choice for the synthesis of a range of dibenzylcalcium complexes directly from CaI_2 and the benzylpotassium reagent. Complex **1**, which can be obtained in the crystalline pure form in large quantities, is the first example of a heavier Ae metal complex with a benzyl ligand [30]. Although stabilized by an α-$SiMe_3$ substituent and by *ortho*-Me_2N–Ae coordination, it is sufficiently reactive to deprotonate a large variety of substrates while being stable enough for convenient handling and long-term storage. In addition, at higher temperatures, it is also fully stable in THF. Replacing the stabilizing α-$SiMe_3$ substituent with an electron-releasing Me group increases the reactivity significantly (**2**) [31]. At a later stage, it was found that the stabilizing *ortho*-Me_2N-substituent can also be removed (**3**) [32]. In contrast to **1** and **2**, $CaBn_2 \cdot (THF)_4$ (**3**) can be

freed from THF under high vacuum. The more reactive Sr analog of **1** is also accessible by the salt metathesis route [33].

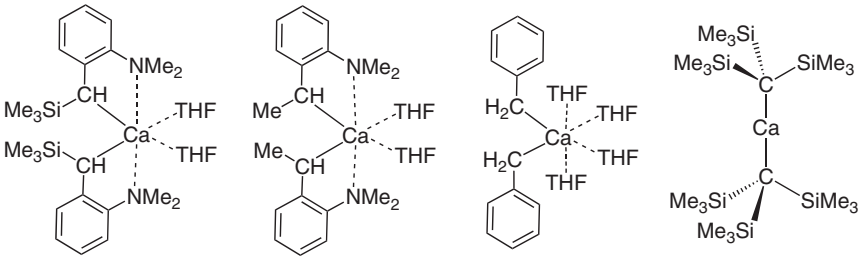

Before this work, dibenzylbarium was prepared in a relatively pure form by a metal–metal exchange method reminiscent of the synthetic protocol for *n*BuNa or *n*BuK: reaction of benzyllithium with $BaN''_2{\cdot}(THF)_2$ resulted in a precipitate of dibenzylbarium and soluble LiN″ [34]. Izod and Waddell reported the syntheses of $[(SrBn_2)_2{\cdot}(THF)_3]_\infty$ and $[(BaBn_2)_3{\cdot}(THF)_4]_\infty$ via salt metathesis [35]. While **3** was crystallized as a molecular complex, the Sr and Ba analogs form polymeric ribbon and sheet structures, respectively. The Okuda and coworkers extended the set of reactive benzylcalcium complexes with the simple bis-allyl complex $Ca(C_3H_5)_2$ which was obtained solvent-free via salt metathesis from allyl potassium and CaI_2 [36].

The synthesis of simple, unstabilized, alkylcalcium complexes was found to be a real challenge. Alkylcalcium complex **4** was prepared by salt metathesis but is hardly reactive on account of steric protection and electronic stabilization of the carbanion center by Me_3Si-substituents [37]. The bis-Me_3Si-substituted alkyl complex $Ca[CH(SiMe_3)_2]_2{\cdot}(dioxane)_2$ was prepared by metal vapor synthesis from Ca^0 and $BrCH(SiMe_3)_2$ [38]. Much later, Hill and coworkers prepared $Ae[CH(SiMe_3)_2]_2{\cdot}(THF)_3$ (Ae = Ca, Sr, and Ba) by the more convenient salt metathesis route [39]. Since the Ph substituent in benzyl complexes stabilizes a carbanion to a similar extent as a Me_3Si-substituent [40], $Ca[CH(SiMe_3)_2]_2{\cdot}(THF)_3$ should have a similar reactivity as **1**. Westerhausen and coworkers isolated the Ca Grignard $(Me_3SiCH_2)CaI{\cdot}(THP)_3$ in which the carbanion is stabilized by only one Me_3Si-substituent [41]. Homoleptic $(Me_3SiCH_2)_2Ca{\cdot}(THP)_4$ was obtained by subsequent salt metathesis with KCH_2SiMe_3 [42]. The THP solvent was used for increased stability. In THF the complex has a half-life time of c. four hours, clearly demonstrating its increased reactivity.

The synthesis of "true" (unstabilized) alkyl complexes of the heavier Ae metals has only been achieved recently. Because this class of compounds is extremely reactive toward polar solvents such as THF, an ether-free synthetic protocol is crucial. Harder and coworkers attempted to prepare unstabilized alkylcalcium complexes by addition of a THF-free amidinate calcium hydride complex to the highly polarized C=C bond in a N-heterocyclic olefin (NHO, Scheme 1.3a). However, instead of isolating an alkylcalcium complex, the

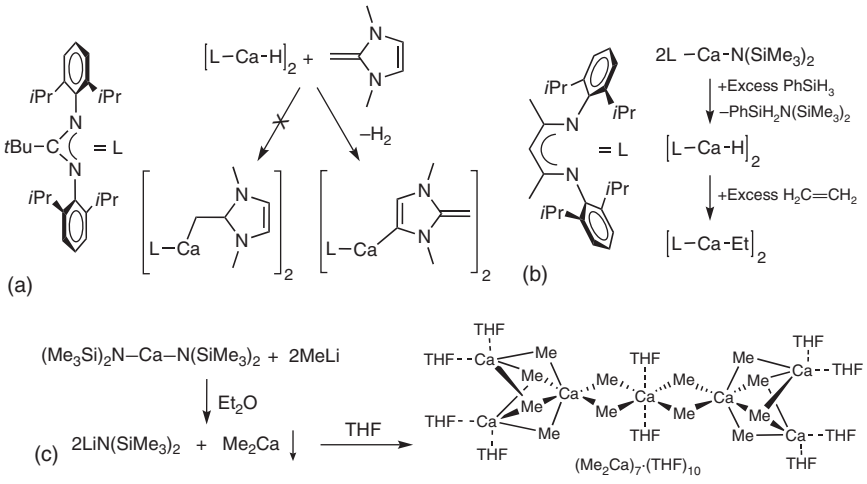

Scheme 1.3 (a) Attempted synthesis of an unstabilized Ca alkyl species. (b) Synthesis of a THF-free Ca hydride complex and further conversion to an ethylcalcium complex. (c) Synthesis of Me_2Ca and its crystal structure from THF.

NHO ligand was deprotonated in the backbone [43]. Attempted synthesis of a THF-free β-diketiminate calcium hydride complex failed because of ligand scrambling and formation of insoluble $(CaH_2)_\infty$ [44], but using excess of $PhSiH_3$, Hill and coworkers successfully isolated the THF-free calcium hydride complex, which formed a highly reactive ethylcalcium complex in reaction with ethylene (Scheme 1.3b) [45]. At the same time, Anwander and coworkers synthesized Me_2Ca by metal exchange between MeLi and $Ca[N(SiMe_3)_2]_2$ in Et_2O (Scheme 1.3c) [46]. The precipitate of $(Me_2Ca)_\infty$ dissolves in THF at low temperatures but also slowly decomposes. Crystals of the larger aggregate $(Me_2Ca)_7{\cdot}(THF)_{10}$ could be isolated.

The Harder group introduced a superbulky β-diketiminate ligand that stabilized a THF-free Sr hydride complex [47]. Reaction with ethylene also formed the first ethylstrontium complex upon polymerization (Scheme 1.4). The very

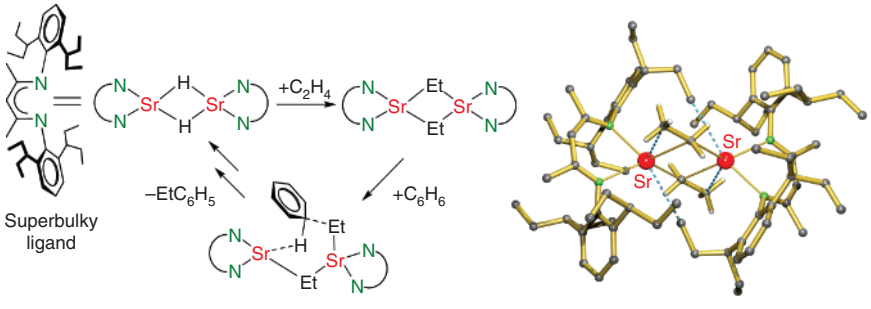

Scheme 1.4 A superbulky β-diketiminate ligand for the stabilization of a Sr hydride complex and synthesis of the first ethylstrontium complex (crystal structure shown). Reaction with benzene gives ethylbenzene.

high reactivity of this complex is demonstrated by its room temperature reaction with benzene, resulting in ethylbenzene and a Sr hydride complex (cf. the ethylcalcium complex shown in Scheme 1.3b reacts with benzene at 60 °C). This formally nucleophilic aromatic substitution likely proceeds through an unstabilized Meisenheimer anion. A similar reactivity observed for the Sr hydride complex is the basis for the Sr-catalyzed deuteration of benzene with D_2.

Apart from these standard methods, procedures that start with Ae metal itself gain popularity. There is some precedence for the direct metal vapor synthesis [38], but there is a lot of room for further development of this technique to activate Ae metals. Unactivated Ae metals may only react with more acidic substrates such as alcohols, but $BaN''_2{\cdot}(THF)_2$ could also be obtained by reacting Ba metal and $HN(SiMe_3)_2$ in THF while bubbling through NH_3 gas to partially dissolve the metal [48]. Also, combinations of methods have been practiced. For example, reaction of Ph_2Hg with Ca and subsequent protolysis of Ph_2Ca with cyclopentadiene formed the calcocene [49]. This redox transmetallation–protolysis (RTP) approach has the advantage of being a one-pot synthesis starting directly from the Ae metal. Highly poisonous mercury reagents have been replaced with the more benign Ph_3Bi redox reagent [50]. Recently, a simple method was reported in which the Grignard reaction of Ae and PhBr produces highly reactive but undefined "PhAeBr" intermediates (Ae = Mg–Ba), which are *in situ* reacted further with organometallic Ae compounds [51]. It is clear that these methods are limited to deprotonation of substrates with pK_a's that are significantly lower than that of benzene. For more comprehensive reviews on preparative group 2 metal organometallic chemistry, see Ref. [52].

1.2.4 Bonding and Structures of s-Block Organometallics

Some trends for the C–metal bond in early main group organometallics are listed in Scheme 1.5. Metal electronegativities decrease down the groups and the highest and lowest values are found for Be (1.57) and Cs (0.79), respectively. Because

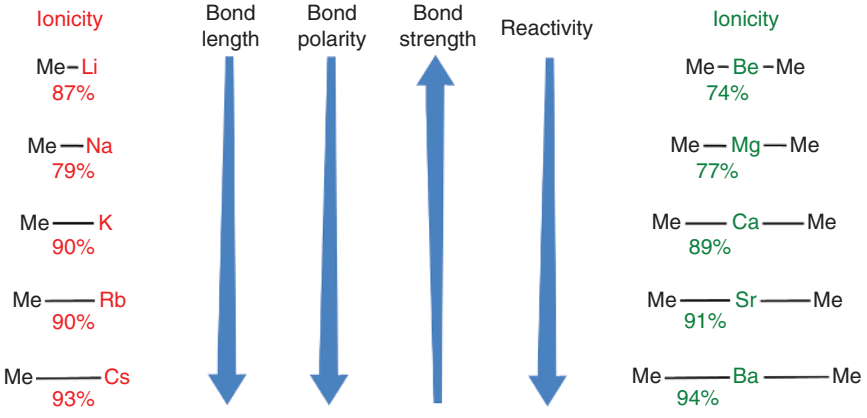

Scheme 1.5 Calculated ionicities of s-block metal–carbon bonds [53] and trends within the groups.

the polarity of the metal–C bond is defined by the electronegativity differences of these bonding partners, the Cs—C bond is among the most ionic one and the Be—C bond has a partial covalent character.

There has been a 25-year long debate on the nature of the C—Li bond. Pauling postulated an empirical formula that expresses its ionicity in terms of electronegativity differences [54], but depending on the scale of electronegativities used, values in the range of 25–50% are calculated. A considerable covalent character was supported by the observation of a substantial ^{13}C–^{7}Li NMR coupling constant of 14.5 Hz for MeLi in diethyl ether [55]. IR studies, however, suggested a considerable ionic character in MeLi based on low frequencies for the H—C—Li bonding [56]. Analyses of NMR chemical shift differences came to the opposite conclusion, estimating only 10% ionicity [55c].

Molecular orbital theory provides precise calculated atomic charges and therefore bond ionicity. Streitwieser described CH_3Li as having essentially no covalent character [57], an extreme viewpoint that was supported by the perfect description of the distorted cubic structure of its tetramer by an electrostatic model using only plus/minus point charges [58]. Lipscomb, however, considered the C—Li bond as being 60% ionic based on high-level calculations using configuration interaction (CI) methods [59]. The problem with atomic charge calculations is that it is not clear where to draw the borderline between C and Li and various methods and/or basis sets give strong contrasting results. The natural population analysis, however, is generally accepted as a method to calculate reliable atomic charges in polar organometallics and is much less sensitive to basis set differences than Mulliken analysis [60]. By the end of 1980s, most key players in the field agreed upon a 80–90% ionicity of the C—Li bond, depending on the organic residue [53].

The very polar nature of early main group metal complexes is the driving force for electrostatic association of monomeric species into larger aggregates. Thus, the simple abbreviation of an organolithium compound by "RLi" is fully inadequate when discussing structures and reactivities. Most student manuals explain the typical tetrameric $(RLi)_4$ or hexameric $(RLi)_6$ with covalent bonding models (Scheme 1.6) using electron-deficient four-center-two-electron models in order to explain bonding. In the light of the predominant ionic nature of the C—Li bond, these representations are far from realistic. These covalent

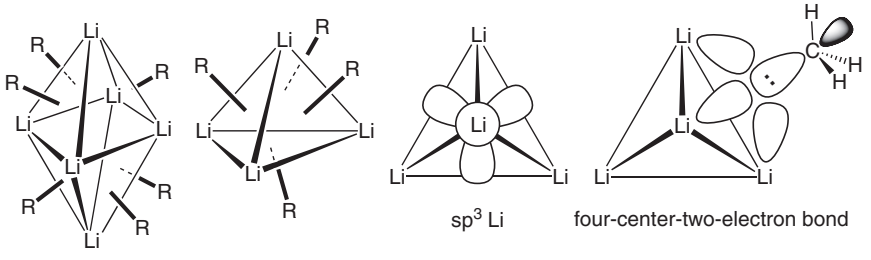

Scheme 1.6 Representations of hexameric and tetrameric organolithium aggregates. Covalent four-center-two-electron bonding model for $(MeLi)_4$ assuming sp^3-hybridized Li and C atoms.

bonding models also falsely suggest the existence of Li—Li bonds, which does not agree with a lack of Li–Li NMR coupling [55b]. From a didactical point of view, ionic bonding models are closer to reality. The polar molecule R^-Li^+ can be seen as a combination of plus and minus charges that interact according to Coulomb's law. Thus, a dimer is the most favorable electrostatic combination of two +/− dipoles for which the total bonding energy can be simply calculated by considering all attractive +/− and repulsive +/+ or −/− Coulomb energies. The distortions from a perfect cube structure for $(MeLi)_4$ have been explained with a fully electrostatic bonding model [58].

Even simpler back-of-a-beer-mat calculations, assuming perfect aggregates with a fixed distance between + and − charges, give a good estimation of the aggregation energy (Scheme 1.7) [61]. These clearly show that a ladder-like trimer is preferred over a cyclic ring and the cube is the most favorable structure for a tetrameric arrangement. The estimated aggregation energies increase with the aggregation number: monomer $-1/r$, dimer $-1.30/r$, trimer $-1.36/r$, tetramer $-1.46/r$, and hexamer $-1.56/r$. This indicates that larger aggregates

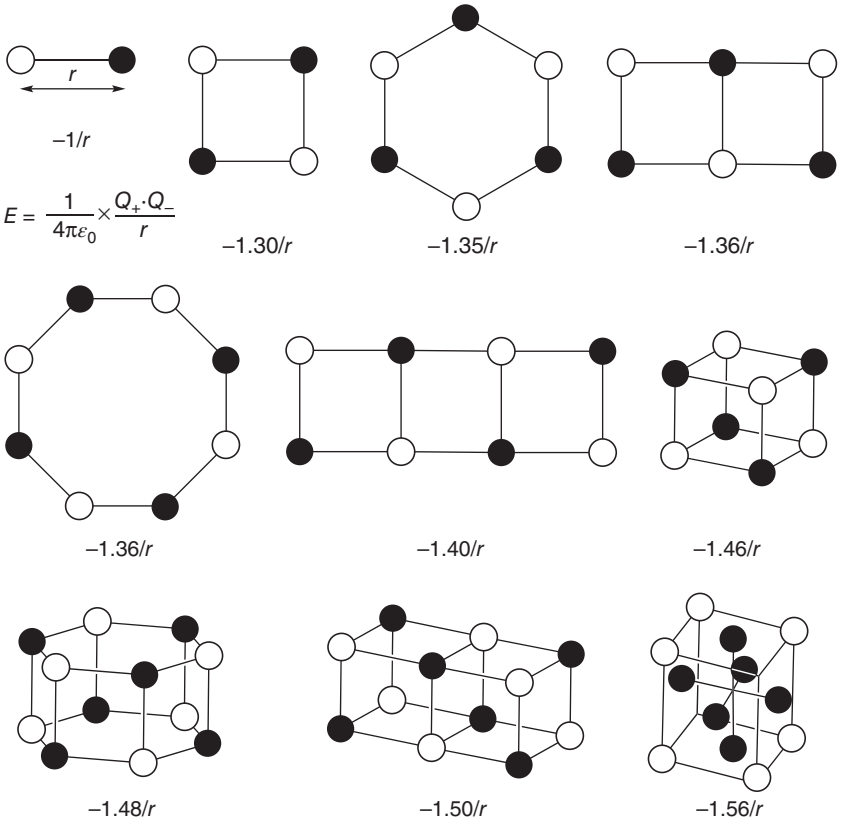

Scheme 1.7 Electrostatic bond energies for combinations of +/− dipoles at a distance of *r*. Following Coulomb's law, the intrinsic energy of one dipole is $-1/r$ au. The electrostatic bond energies for the aggregates (given per dipole) are calculated by considering all attractive (+/−) and repulsive (+/+ and −/−) interactions.

are always more stable than smaller ones. Calculation of an "endless" rock salt structure would converge to an aggregation energy of $-1.748/r$ per dipole, a number which is also known as the Madelung constant. The reason why MeLi is tetrameric and does not form a rock salt structure in the solid state is the nonspherical distribution of negative charge in the Me^- anion. Although the spherically symmetric Cl^- anion can interact with Na^+ in all directions, the hydrogen atoms in CH_3 limit its interaction with the neighboring aggregates, which explains the formation of discrete tetramers. However, in the solid state, there are also important interactions between $(MeLi)_4$ clusters: each Li corner interacts with the Me groups of neighbors with C· · ·Li distances of c. 2.52 Å and vice versa (Scheme 1.8). Although only slightly longer than the C—Li bond of c. 2.28 Å within the tetramer, the interaggregate bonding is considerably weaker than the intra-aggregate bonding because the center of negative charge does not coincide with the C nucleus. The 3D interaggregate linking is still strong enough to make $(MeLi)_4$ fully insoluble in nonpolar solvents. In ethers, however, it dissolves well and maintains its tetrameric structure in which the Li corners are solvated by ether. Increasing the size of the carbanion also increases the interaggregate bonds. Ethyllithium crystallizes as tetrameric aggregates that are only interlinked in two dimensions. The 2D layer structure is shielded on top and bottom by the Et groups and the differences between the intra-aggregate C—Li bonds (2.31 Å) and interaggregate C· · ·Li (2.53 Å) distances is similar to that in MeLi. Because of less extensive interlinking, EtLi is soluble in aromatic solvents but not in hexane. Increasing the size of the carbanion from Et^- to tBu$^-$ fully blocks interaggregate interactions. Consequently, $(t\text{BuLi})_4$ is very well soluble in pentane and even sublimes under vacuum. This clearly shows the enormous influence of nature and size of the carbanion on the structures of organolithium complexes and inherently on their physical properties. Because the cation–anion ratio is decisive, changing Li^+ for the larger cations Na^+ and K^+ will have the same effect as reducing the size of the carbanion. Consequently, Na and K complexes often show pronounced polymeric structures and are less soluble with increasing cation size.

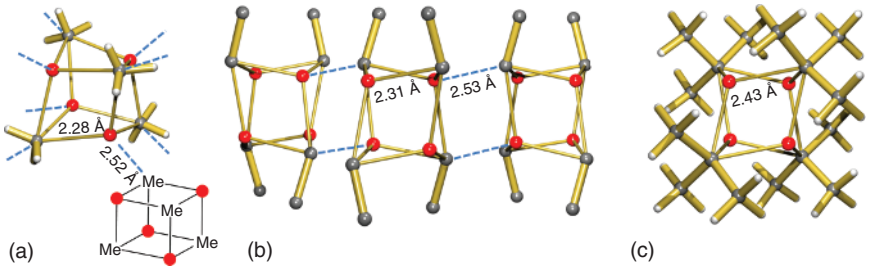

Scheme 1.8 Crystal structures of (a) $(MeLi)_4$ with 3D network, (b) $(EtLi)_4$ with 2D network (H atoms not shown). The 2D plane is shielded on both sides with ethyl groups. (c) $(t\text{BuLi})_4$ is fully shielded.

Group 2 organometallic complexes follow the same bonding principles and their structures can also be thought of as electrostatic combinations of plus and

minus charged ions. Bonding to the lightest metal in the group, however, has significant covalent contributions. This can be seen in the structures of Ae metal hydrides AeH_2. The heaviest hydrides (Ca, Sr, and Ba) feature ionic 3D salt structures with a $PbCl_2$ lattice (coordination numbers: Ae = 9, H = 4 and 5), and MgH_2 crystallizes with a rutile lattice (coordination numbers: Mg = 6, H = 3). In contrast, the structure of BeH_2 is often described as the linear polymer $[Be(\mu\text{-}H)_2]_\infty$ (coordination numbers: Be = 4, H = 2) in which Be is sp^3 hybridized and hydrogens are bonded through electron-deficient three-center-two-electron bonds, i.e. a structure with strong similarities to that of B_2H_6. More accurate studies, however, present a 3D network structure of corner sharing BeH_4-tetrahedra (**5**) [62].

Because group 2 organometallics are constituted of two shielding carbanions per metal center, there, is in contrast to group 1 metal chemistry, a much smaller tendency to aggregate to larger complexes. Consequently, the vast majority of all Ae metal complexes is present as a monomer. Dimeric aggregates with μ^2-bridging carbanions are also plentiful, but μ^3-bridging carbanions are rare and usually only found for complexes with smaller anions such as Me^- [46] or with larger Ba^{2+} cations [63].

The tendency of anions to bridge metal centers increases from $R_3C^- < R_2N^- < RO^-$. Amides are either terminally bound or tend to bridge in μ^2-fashion, which is clearly demonstrated by the structures of $(AeN''_2)_2$ that are dimeric over the whole range (Mg–Ba) (**6**) [48, 64]. There are many examples of Ae alkoxide complexes with μ^3-RO^- anions and also spherically symmetric halogenide anions display strong bridging tendencies that increase from I^- to F^-. The highest coordination numbers have been found for O^{2-} and H^- anions, which, as part of a complex, show up to μ^6-bridging [65, 66].

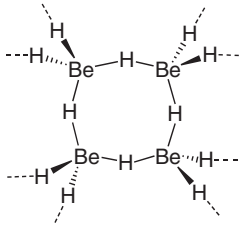

5

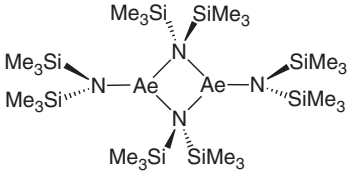

6 Ae = Mg, Ca, Sr, Ba

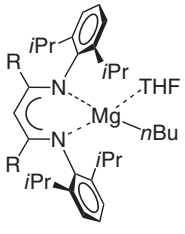

7a R = Me
7b R = *t*Bu

Aromatic groups (or other functionalities rich in π-electrons) also show great potential to involve in metal coordination. These ligands especially bind to the larger softer metal cations. Ba complexes often crystallize with coordinated benzene ligands (even despite the presence of THF) [63]. The importance of weak secondary interactions on structure and stability of Ae complexes are becoming increasingly clearer [67]. These interactions are electrostatic in nature and rely heavily on metal-induced polarization. Consequently, they are more pronounced for complexes with Ae^{2+} cations than for alkali metal complexes with a singly charged cation. Apart from interactions with π-electron density [68], Ae complexes often feature strong agostic metal· · ·H–C interactions. Although the

original definition of an agostic interaction is specifically related to intramolecular three-center-two-electron M—H—C bonding with transition metals in which $d(M) \rightarrow \sigma^*(C–H)$ back-donation is part of the bonding description, the wording for early main group metals is arguably not correctly chosen [69]. There are indeed clear differences in geometry or effects on NMR chemical shifts, and therefore for s-block metals, the new definition "anagostic interaction" would be more appropriate. Because early main group metals do not possess partially filled d-orbitals, the anagostic interaction is of different nature and best described by polarization of a C—H bond (or CH_3 group) by the positively charged Ae^{2+} cation, creating an attractive electrostatic force between the positive point charge and the induced dipole. Especially, $Ae^{2+}\cdots Me^{\delta-}–Si^{\delta+}$ interactions are strong and can often be witnessed in $Ae–N(SiMe_3)_2$ complexes [44, 64, 70]. Because of the low electronegativity of Si, strong $Ae^{2+}\cdots H^{\delta-}—Si^{\delta+}$ bonding contributes to the stability of complexes with the Anwander $N(SiMe_2H)_2$ ligand [71]. Fluorinated ligands or substituents can also interact with metal centers via electrostatic $Ae^{2+}\cdots F^{\delta-}–C^{\delta+}$ contacts, thus filling the metal's coordination sphere [67, 68, 72].

For more detailed information on the structures of group 2 metal complexes, the reader is referred to Ref. [52].

1.2.5 Dynamics of s-Block Organometallics in Solution

The solubility of early main group metal complexes strongly depends on saturation of the metal's coordination sphere. Whether the species is monomer or aggregated, large anionic and/or neutral ligands can block the metal for further intermolecular (or interaggregate) interactions, thus increasing its solubility in apolar solvents. For solubilization of complexes with smaller ligands, often polar ethereal or amine solvents are crucial. Because of the higher number of anionic ligands, group 2 metal complexes are generally better soluble than the alkali metal compounds. Because the coordination sphere of larger metals is more difficult to saturate, solubilities decrease with increasing metal size.

Highly aggregated organolithium compounds display fascinating dynamics in solution. The very rapid metal exchange processes within or between aggregates originate from the ionic nature of the bonds. Weak, mainly ionic, bonds to Li^+ are exploited in the well-known Li batteries for which fast dynamics of the Li^+ cation are essential. The observation of $^{13}C–^{7}Li$ NMR coupling facilitated investigations on the aggregation state and dynamics of organolithium compounds tremendously [73]. Because of the much lower quadrupole moment and spin quantum number of ^6Li ($I = 1$), studies of $^{13}C–^6Li$ NMR coupling are even more informative [74]. The multiplicity of the ^{13}C signal not only reveals the number of ^6Li bonding partners (Scheme 1.9) but information can also be extracted from the NMR chemical shift or the coupling constant, which decreases with increasing number of ^6Li contacts [75]. Because of the highly dynamic nature of Li complexes, NMR samples often have to be cooled to observe these coupling patterns. At higher temperature, fast exchange between aggregates gives a singlet signal. Lowering the temperature freezes interaggregate exchange, but fast exchange within the aggregate allows for coupling with all Li nuclei. Further cooling results in static bonding, reducing the multiplicity. The presence of

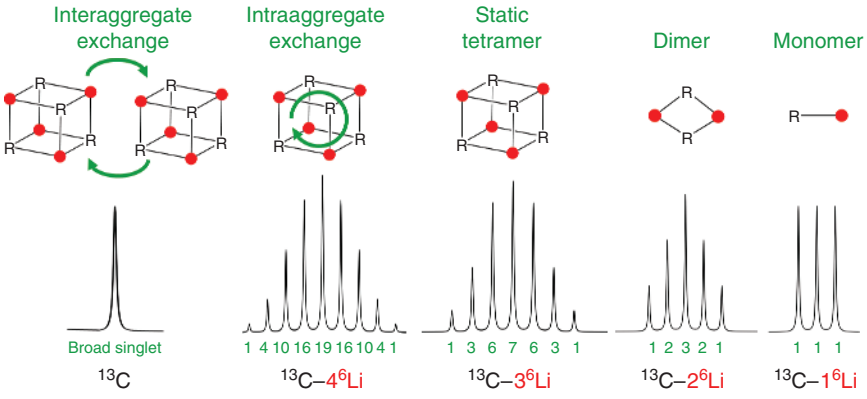

Scheme 1.9 ^{13}C NMR coupling with ^{6}Li ($I = 1$) gives information on dynamics and the aggregation state.

equilibria between aggregates (tetramer–dimer–monomer) reduces the splitting further but increases the coupling constants from c. 5 to 18 Hz. The rate of these exchange equilibria decides whether coupling constants can be detected ($\Delta G^{\ddagger}$ can vary between c. 5 and 25 kcal/mol) [76]. Polar solvents generally accelerate exchange processes and lower the aggregation number. *n*BuLi, which is a hexamer in hexane, is dissolved in THF in a tetramer–dimer equilibrium. Rapid injection NMR studies have shown that the dimers in this mixture react at least 4 orders of magnitude faster with an aldehyde than the tetramers [77]. The higher reactivity of smaller aggregates partially explains why polar solvents accelerate organolithium reactions.

Unfortunately, the favorable magnetic properties of Li are unique for the s-block metals, and these highly useful NMR methods are limited to studies on organolithium compounds. There are, however, other methods that can be used to gain information on aggregation. Cryoscopy, a technique that can determine the molecular weight of a dissolved molecule by measuring the solvent's melting point lowering, has been used successfully in organolithium chemistry, but in the case of equilibria, it always gives an averaged molecular weight [78]. Recently, diffusion-ordered NMR spectroscopy (DOSY), a technique that determines molecular weight by measuring diffusion rates, has been introduced to s-block metal chemistry [79]. This technique is becoming an increasingly popular method to extract information of s-block organometallics in solution.

As bonds to the twofold positively charged Ae^{2+} cations are stronger than those to group 1 metal cations, the dynamic processes for Ae metal complexes are slower. This is nicely illustrated by water ligand exchange rates for their hydrated cations, which increase with a decrease in the cation's surface–charge area [80]. The fastest exchange rate is found for metal ions of large ionic radius and with a low charge. Exchange rates for the alkali metal cations are among the fastest and vary roughly from 10^8 s^{-1} (Li^+) to 10^{10} s^{-1} (Cs^+), whereas exchange at Ae^{2+} cations is much slower varying from 10^6 s^{-1} (Mg^{2+}) to 10^9 s^{-1} (Ba^{2+}); the very small Be^{2+} has a very slow exchange rate of 10^3 s^{-1}. Ligand exchange at s-block

metal cations is generally much faster than that at transition metals, a property that is certainly advantageous in catalysis.

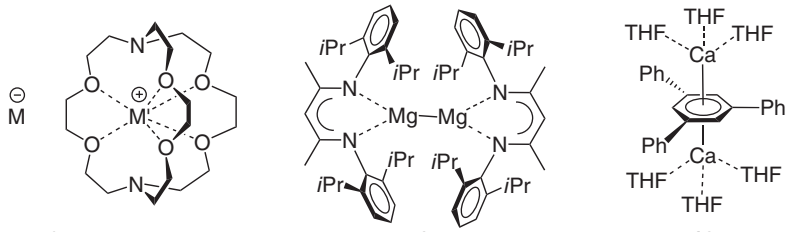

8 **9** **10**

Chisholm and coworkers reported an in-depth study on THF exchange rates in two β-diketiminate Mg complexes that vary in bulk (7) [81]: in **7b**, the larger *t*Bu backbone substituents create larger metal shielding by forcing the aryl groups to bend toward the metal. Although the less shielded Mg in **7a** can exchange THF in an associative process, solvent exchange in the sterically encumbered **7b** is considerably slower and purely follows the more difficult dissociative route ($\Delta H^{\ddagger} = 7.0(5)$ kcal/mol, $\Delta S^{\ddagger} = 11.6(4)$ cal/mol).

Although ligand exchange processes in Ae metal complexes are slower than for group 1 metal complexes, group 2 metal chemistry is complicated by another serious problem: the Schlenk equilibrium. Originally discovered by Wilhem Schlenk Jr., who wrote his dissertation on this subject under supervision of his father Wilhem Schlenk Sr., the Schlenk equilibrium has been formulated for ligand exchange processes in Grignard reagents: $2RMgX \rightleftharpoons R_2Mg + MgX_2$ [4, 25]. In Et_2O, this equilibrium lies slightly toward heteroleptic RMgX (two different ligands), whereas for the more polar, less bulky, solvent THF, predominantly homoleptic species (equal ligands) are observed. Density functional theory (DFT) calculations are in agreement with this observation and attribute this difference to the fact that the less bulky THF solvent especially stabilizes MgX_2 by coordination of up to four THF ligands [82]. Recent *ab initio* molecular dynamics calculations on MeMgCl in THF give detailed insight into these ligand exchange processes and underscore that the solvent is a direct key player (Scheme 1.10) [83]. The most stable dimer is bridged by two Cl^- anions, but the

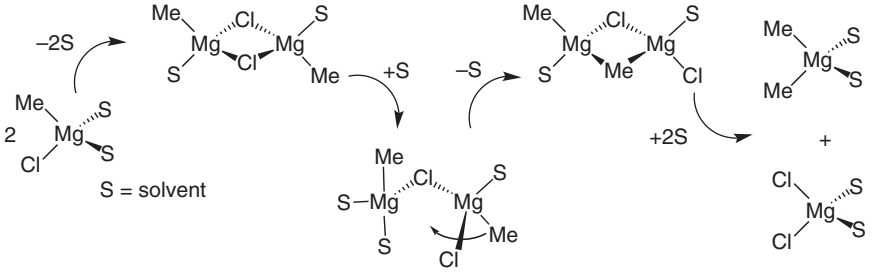

Scheme 1.10 Solvent dynamics play a crucial role in ligand exchange by the Schlenk equilibrium [83].

four-membered Mg_2Cl_2 ring can open up by filling empty coordination sites with a solvent ligand illustrating that polar solvents support these dynamics.

This equilibrium between heteroleptic and homoleptic complexes becomes increasingly faster and more problematic for complexes with larger Ae metals, especially when dissolved in polar solvents. Schlenk equilibria, however, also exist for monomeric heteroleptic complexes in nonpolar solvents. These mechanisms are less well understood but because of the lack of polar solvents to stabilize free coordination sites it is likely that such processes follow an associative pathway. Therefore, open coordination sites should be avoided. For this reason, strongly coordinating multidentate bulky ligands can stabilize heteroleptic complexes of heavier Ae metals [84] but need to be bulkier with increasing metal size [47, 85]. It seems possible to also stabilize heteroleptic complexes with a combination of electron-withdrawing and electron-releasing ligands [72], but clearly, more research is needed to understand and prevent ligand exchange processes.

1.2.6 Low-Valent s-Block Chemistry

In contrast to the late main group metals, the chemistry of the s-block elements has always been characterized by the metal's distinct oxidation state that equals the group number. Apart from the metallic state, there are hardly exceptions to the alkali metal +I and Ae metal +II oxidation states. One of the few exceptions is the −I oxidation states of the alkali metals in an alkalide salt, which is a combination of a metal anion and a metal cation stabilized by a crown ether of cryptand (e.g. **8**) [86]. The energy gained by cation complexation is the driving force for electron transfer from one alkali metal to the other alkali metal. The negatively charged metal can be the same or preferably should be more electronegative than the positively charged metal.

For the Ae metal Mg, there is a rich chemistry in its subvalent form Mg(I) [87, 88]. Although Mg(I) species have been detected in outer space or could be isolated at low temperatures in a matrix, Jones and coworkers reported in 2007 the first examples of a Mg(I) complex stabilized against disproportionation by a bulky bidentate amidinate or β-diketiminate ligand (**9**) [89]. Meanwhile, a large variety of these Mg—Mg bond complexes have been isolated, mainly with the conveniently tunable β-diketiminate ligand. These electron-rich complexes can be used as reducing agents that are soluble, selective, and safe, allowing for facile control of stoichiometry, thus avoiding overreduction. They have been the key to isolation of several novel compound types that could not be prepared using conventional reducing agents (e.g. K mirror or KC_8) [88]. Similar complexes with heavier Ca could hitherto not be obtained, probably on account of the weaker Ca—Ca bond and more facile disproportionation. Surprisingly, the lighter Be–Be complexes have also not been isolated. It is likely that these exist as persisting radicals that decompose via a different pathway.

Westerhausen and coworkers reported a serendipitous example of a Ca(I) complex (**10**) [89]. Several observations support the assumption that the triphenylbenzene moiety is doubly negatively charged, that the formal oxidation state of Ca is +I, and that there are no hidden hydride or other anions. Charge calculation

by the natural population analysis (NPA) resulted in +1.03 charges for the Ca atoms and consequently −1.94 for the arene, and analysis of the THF-solvated molecule led to a charge of −3.68 at the arene and +1.84 charges at the Ca atoms. This has been attributed to stabilization of a high positive charge at the metal by the THF ligands and would better fit for Ca in the oxidation +II. The challenge to isolate an unequivocal Ca(I) complex with a Ca—Ca bond is still open.

1.3 s-Block Organometallics in Catalysis

In classical organic syntheses, early main group organometallics have traditionally been the highly reactive nucleophiles or Brønsted bases. It is only since the start of this century that they emerged as catalysts for a growing variety of transformations [23]. This development is strongly motivated by the search for replacement of precious metals by more abundant elements. Although the cost factor is often mentioned as an advantage for doing catalysis with metals that do not belong to the platinum group ("cheap metals for noble tasks" [90]), the generally higher catalyst loadings and also the price of the ligand as well as recyclability should be considered. The worldwide availability of most early main group metals is therefore a much stronger argument for their application. This avoids price instabilities by monopoly situations and is especially for industries an important consideration for long-term investments.

Another major advantage for most s-block metals is their superb biocompatibility. Calcium, the fifth most abundant element in the earth's crust [91], is present in large quantities in the human body. Avoiding the more harmful metals such as Pt is in particular for the pharmaceutical industry, in which catalysis plays a key role, an important issue. These driving forces have motivated chemists from different backgrounds to investigate s-block metal catalysis. There seems to be two schools of investigators: the organic chemists generally focus more on Lewis acid catalysis centered mainly at the metal cation, whereas the inorganic (or organometallic) researchers exploit the strongly basic and nucleophilic properties of the anionic part or the combined organometallic species. Although addition to an unsaturated bond can be described either from the cationic or the anionic side, the majority of catalytic reactions are likely a combination of both, strongly depending on the extent of Lewis acidity and nucleophilicity (Scheme 1.11). Supposing that these areas complement and support each other, the current book describes examples of both schools.

1.3.1 Working Principles in Lewis Acid Catalysis

Chapters 11 and 12 deal with Lewis acidic early main group metal catalysis (some recent reviews are listed in Ref. [92]). For example, Niggemann and coworker focused mainly on the development of the highly Lewis acidic Ca^{2+} cation, working with a system consisting of Ca^{2+} and the weakly coordinating anions Tf_2N^- (Tf = $CF_3S(O)_2O$) and PF_6^- [92a]. The anions are merely present as innocent spectators and the Lewis acidic Ca^{2+} cation is the active part of the catalyst.

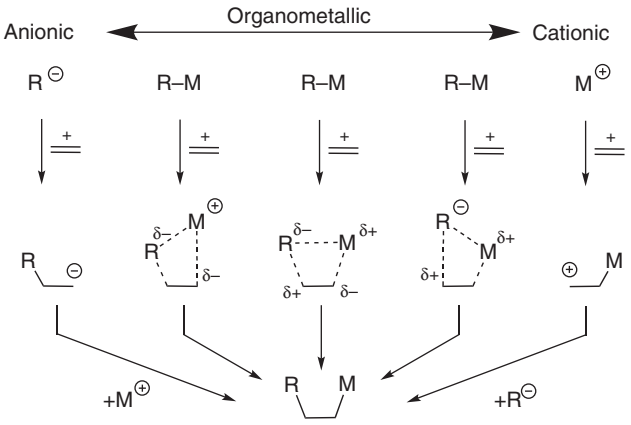

Scheme 1.11 The continuous transition from nucleophilic to electrophilic addition to an unsaturated bond.

Some selected examples of cation–substrate activation by pure electrostatics are shown in Scheme 1.12. Early calculational studies demonstrated that polarized double bonds such as C=O or C=N are strongly activated for nucleophilic attack by cation coordination [93]. This mode of electrostatic activation is general for any C—X bond and also holds for C=C bonds, which will be discussed in detail in Section 3.3. Another mode of substrate activation is demonstrated by ROH coordination. The metal Lewis acid is not only the key to generation of highly reactive carbocations, it could also bind an alcohol leading to polarization and acidification of the O—H group causing facile loss of H^+ which itself could be a catalyst. Cases of assumed "transition-metal-catalyzed" reactions have been shown to be H^+ catalyzed [94]. It is likely that "hidden Brønsted catalysis" also plays a major role in many Lewis acid-catalyzed reactions, especially as it is known that traces of water are often essential for catalytic activity. This topic is discussed in greater detail in Chapter 11. Notwithstanding the fact that the "true" catalyst may be a simple proton, the activating influence of Li^+ or Ca^{2+} cations has been substantiated by calculation and this concept of activation likely plays an important role in biological oxidation [95].

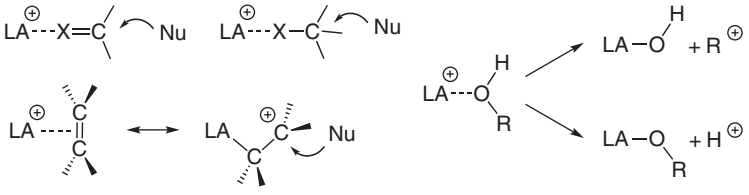

Scheme 1.12 Selected examples of Lewis acid (LA) substrate activation.

Truly cationic Lewis acidic catalysis (i.e. without marked influences of the anion) cannot be controlled by the anion. However, the metal cation can be modified by addition of neutral ligands that can control its sterics and electronics. This is especially exploited in enantioselective Lewis acid catalysis

and exemplified by numerous transformations typically catalyzed by acids or metal cations: e.g. cycloadditions, ring-opening reactions, (hetero)-Diels–Alder, Mannich- or Michael-type, Aldol condensations, or Friedel–Craft reactions. In Chapter 12, Kobayashi and coworkers specifically focus on enantioselective Lewis acid catalysis.

1.3.2 Working Principles in s-Block Organometallic Catalysis

The majority of the catalytic reactions described in this book are of organometallic nature, i.e. the anion and metal cation operate in concert (Scheme 1.11). These reactions can be much easier controlled by ligand design. This is especially true for group 2 metal catalysts L–Ae–R that are often build up from a passive spectator ligand (L) and a reactive group R. In contrast to transition metals, which show fast and reversible switching of oxidation states, the early main group metals generally favor only one oxidation state. This excludes catalytic pathways with redox steps such as oxidative addition and reductive elimination. In this respect, s-block metal catalysis has strong similarities to lanthanide metal catalysis for which redox reactions also do not play a role. This simplifies the possible steps enormously, and most catalytic cycles are built around basic dipolar transformations such as deprotonation/protonation, addition/elimination, nucleophilic substitution, or nucleophilic ring opening. Most of the catalytic reactions can be classified as (hetero)functionalization of unsaturated bonds including hydrogenation, hydroboration, hydrosilylation, hydroamination, or hydrophosphination. These all follow the same simplified protocol shown in Scheme 1.13a: catalyst initiation and substrate coordination is followed by addition and nucleophilic substitution. This kind of reactivity is extensively described in Chapters 3–5 (hydroamination and hydrophosphination), Chapter 6 (hydrosilylation), Chapter 7 (hydrogenation), and Chapter 8 (hydroboration). It is important to note that the substrates X–Y react in a dipolar manner. For example, in alkene hydrogenation, the H_2 molecule reacts protic (H^+) and hydridic (H^-). This means that for hydrogenation, hydroboration, and hydrosilylation, the catalytic active species could be a metal hydride species.

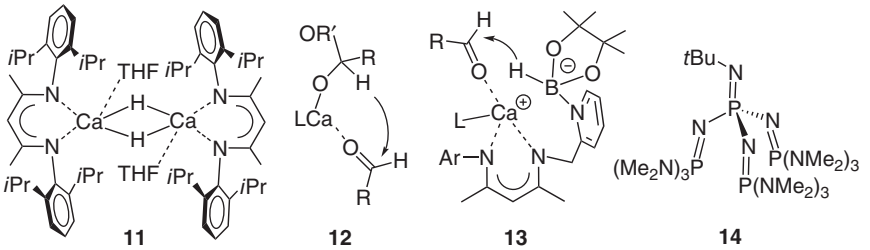

Metal hydride complexes of group 1 and 2 metals have been oddities for a long time. Their intermediacy in catalytic cycles, however, accelerated research in this area tremendously and after isolation of the first calcium hydride complex (**11**) lately several review articles on s-block metal hydrides have appeared [96]. Intermediate metal hydride species also likely play a role in dehydrogenative coupling

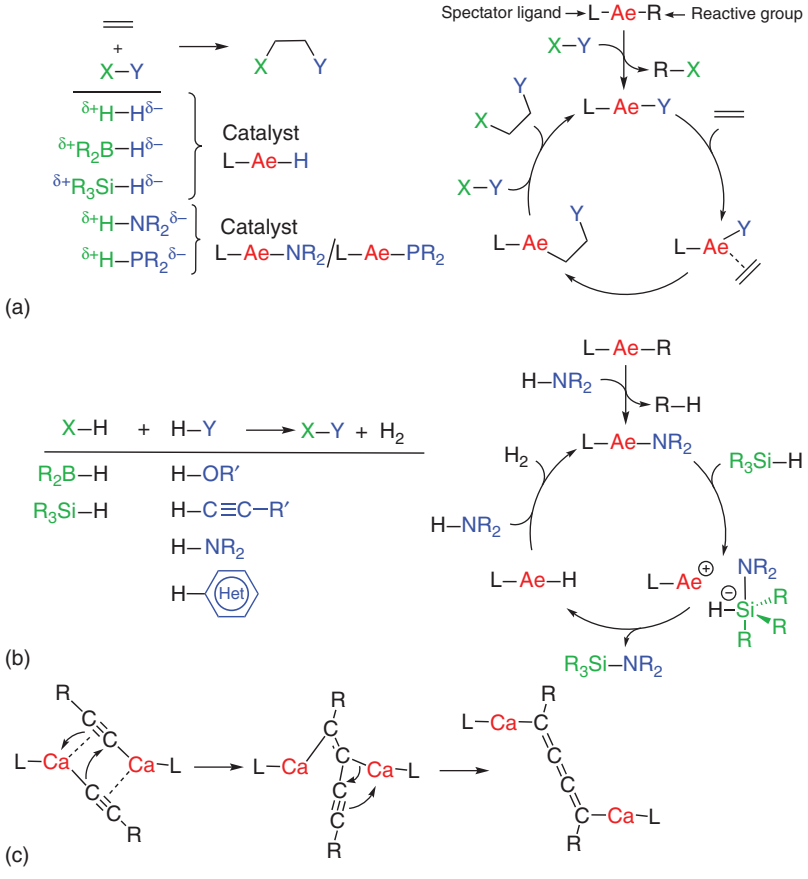

Scheme 1.13 (a) General mechanism for hydrogenation, hydroboration, hydrosilylation, hydroamination, and hydrophosphination of unsaturated bonds using catalyst L–Ae–R. (b) General mechanism for dehydrogenative cross-coupling exemplified by the cycle for amine hydrosilylation. (c) An unusual example of anion–anion coupling.

reactions, which is another group of transformations that follows a collective mechanism (Scheme 1.13b). In this case, the catalyst is formed by deprotonation of the substrate, which, after a substitution reaction with a borane or silane, forms a hydride that in reaction with relatively acidic substrates produces H_2, regenerating the catalyst. Depending on the substrate, these reactions can be much more complicated, and this subject is extensively discussed in detail in Chapter 9. The recent dehydrogenative silylation of C—H bonds in aromatic heterocycles shows that also less acidic substrates can be converted, but the mechanism may be of the radical type [97].

Chapter 2 discusses application of s-block organometallics in polymerization chemistry which involves standard reactivity such as nucleophilic ring opening or successive addition reactions. Finally, Chapter 13 describes miscellaneous reactions in which the metal catalyst shows a different reactivity. For example, in the Ca-catalyzed Tischtschenko aldehyde dimerization, hydride transfer

from an alcoholate to an aldehyde proceeds through combined β-hydride elimination/addition reaction (**12**) [98]. Another case of such reactivity was recently postulated for aldehyde hydroboration using a catalyst without a highly reactive group. Instead, the pendant pyridine ring assists in creating a hydridic borate that directly transfers the hydride to the aldehyde (**13**) [99]. This concept differs from hydroboration according to Scheme 1.13a in which metal hydride intermediates are proposed. A recent report on ketone hydroboration with an amidinate Ca iodide catalyst may also follow a hydride-free route, which would explain its unusually highly functional group tolerance [100]. Harder and coworkers suggested similar hydride-free routes for the Mg-catalyzed pyridine hydroboration and proposed direct transfer of the hydride from borate to pyridine [101]. This conclusion was based on differences in regioselectivity between the stoichiometric reaction of an Mg hydride complex with pyridine and its catalytic reactivity.

An odd case of C–C coupling of alkynide carbanions is described by Hill and coworkers (Scheme 1.13c) [102]. This reaction represents the unusual nucleophilic attack of an alkynide anion at another alkynide anion. The driving force is likely the formation of an extended C=C=C=C system. Also, side-on coordination of the alkynide anion to Ca^{2+} may be important to C≡C bond activation.

1.3.3 Substrate Activation by s-Block Metals

Because early main group metals do not possess partially filled d-orbitals for substrate activation by $d \rightarrow \pi^*$ back-bonding, it is questionable to what extent the metal plays a role in the mechanism. Alkene–metal coordination is well established in transition metal chemistry, but for the main group metals, examples are scarce [67, 103]. Metal· · ·C distances are long and bonds should be considered weak [104]. This raises the question: how important is the metal in s-block metal catalysis? The Harder group reported a series of investigations that scrutinize the role of the metal [105]. The metal in an s-block metal amide complex was simply replaced by the Me_4N^+ cation. It was found that the salt $[Me_4N^+][Ph_2N^-]$ catalyzes the hydroamination of carbodiimides equally well as the Ca catalyst $Ca[N(SiMe_3)_2]_2$, thus approaching the anionic limit in Scheme 1.11. DFT calculations, however, show that Me_4N^+ is not truly noncoordinating and also has a minor activating effect on the C=N bond, albeit much less than that of the Li^+ cation in the model catalyst $LiNPh_2$ (Scheme 1.14a). The conclusion is that for highly activated C=N bonds in a carbodiimide, activation by metal–substrate coordination is rather unimportant. On the other hand, the "naked" anion catalyst did not perform in the intramolecular alkene hydroamination, which runs smoothly with $Ca[N(SiMe_3)_2]_2$ (Scheme 1.14b). This was attributed to the low basicity of the Ph_2N^- anion and therefore the same reaction was reinvestigated with a strong neutral metal-free organic base: the Schwesinger base P4 (**14**). Only under harsh conditions (90 °C, five days), substrate conversion was observed, but although the catalyst P4 was able to deprotonate the substrate, the reaction followed a different course. The absence of ring closure suggests that alkene activation by metal coordination plays a crucial role. Indeed, addition of a catalytic

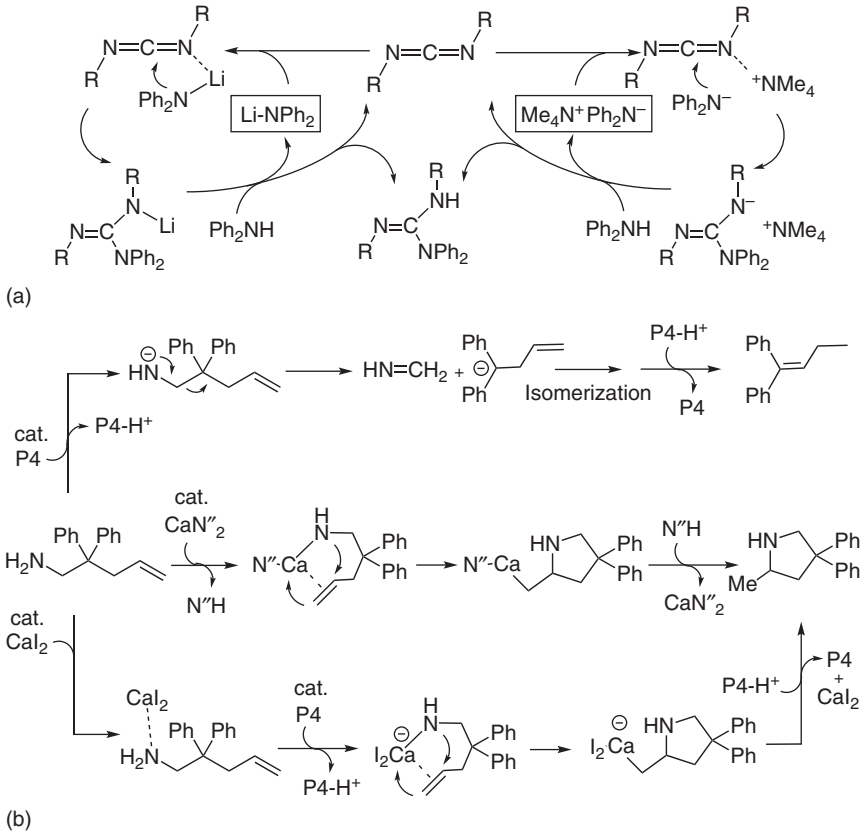

Scheme 1.14 (a) Hydroamination of carbodiimide catalyzed by $LiNPh_2$ (left) or by $[Me_4N^+][Ph_2N^-]$. (b) Intramolecular alkene hydroamination catalyzed by CaN''_2 (N″ = $N(SiMe_3)_2$) or by the P4/CaI_2 combination. Reaction with only P4 gives a different product.

quantity of CaI_2 to a P4/aminoalkene mixture formed the ring closure product under mild conditions (25 °C, two hours). It is suggested that Ca^{2+}-aminoalkene coordination acidifies the NH_2 group, facilitating its deprotonation and that Ca^{2+}-alkene coordination activates the C=C bond enabling smooth ring closure. This hybrid catalyst, consisting of a neutral organic base and a metal salt, offers ample opportunities for variation. Most importantly, it clearly demonstrates the activating influence of the metal cation.

Given the importance of the metal cation in alkene functionalization, Harder and coworkers studied the details of early main group metal coordination to unsaturated substrates [68, 106]. The goal was to isolate a Lewis base-free cationic Mg complex with an open space for substrate coordination. In cationic complex **15**, the Mg metal interacts with the weakly coordinating borate anion (Scheme 1.15). Addition of aromatic solvents partially breaks the cation–anion contacts and a tightly bound Mg–(η^3-benzene) complex (**16**) is formed. In the presence of EtC≡CEt, the first unsupported Mg–alkyne complex (**17**), which also persists in solution, is formed. Compared to the neutral Fe(I)–alkyne

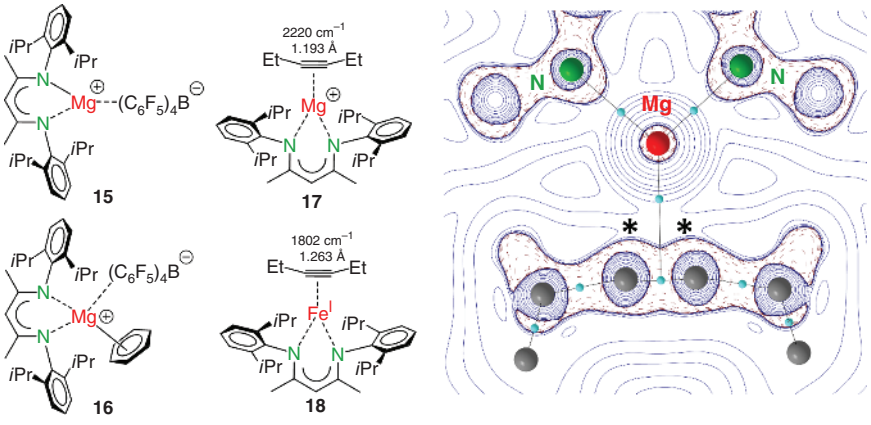

Scheme 1.15 A cationic β-diketiminate complex with a nearly "naked" Mg cation (**15**) binding benzene (**16**) or alkyne (**17**). The inset shows an AIM representation of the Laplacian of the electron density in **17**: π-electron density is polarized toward Mg (see *).

complex (**18**) [107], the triple bond in the Mg complex is hardly stretched, but the lowering of the C≡C stretching frequency by 40 cm^{-1} compared to free EtC≡CEt (2260 cm^{-1}) is significant. The Et substituents are bent by c. 11° away from the C≡C axis, thus shifting electron density toward the metal. This can be clearly seen in an atoms-in-molecules (AIM) representation of the Laplacian of the electron density in **17**, which shows polarization of alkyne π-electron density toward Mg^{2+}. Ion-induced polarization is particularly strong for asymmetrically bound substrates, which polarizes the C≡C bond also along its axis [104], leading to nucleophilic attack. The power of this type of substrate activation has been recently demonstrated by the dearomatization of benzene, which was activated by a similar cationic Ca complex [108].

1.3.4 Future of Early Main Group Metal Catalysis

s-Block metal catalysis experienced a rapid development in the past two decades. This is especially true for the group 2 metals. Transformations typical in transition metal catalysis now routinely can be mediated by early main group metals and it is to be expected that the field will steadily grow further.

Hitherto, enantioselective transformations have been found to be very challenging. In contrast to transition metal catalysts, which have defined coordination geometries that are dictated by orbital interactions, ionically bound s-block metal catalysts are highly dynamic and exercise much less control over diastereoselective transition states. Because both enantioselective catalysis and replacement of benign and expensive platinum group metals are especially important for the pharmaceutical industry, further development of this field is highly desirable. Development of ligand systems that do not allow for much fluxionality may be the key to improve ee values.

At the same time, functional group tolerance is crucial for a wider application of s-block metal catalysts. The recently presented unstabilized Ae metal alkyl

species of the heavier metals Ca and Sr [45–47] may display unique reactivity but are too reactive to cope with the many functional groups in complicated pharmaceutical building blocks. Broader functional group tolerance may be achieved with more covalently bound Mg complexes and less reactive alkoxide or amide ligands.

Secondary interactions between ligand and metal become increasingly more important to stabilize complexes [67, 71]. Ligand–substrate secondary interactions could, similar to that in organocatalysis, also play a role in catalysis. There are cases of "organocatalysis" in which Ca^{2+} that leached from the silica column used in catalyst "purification" has been shown to be essential [109]. The possibilities of such inorganic/organic hybrid catalysts are hitherto largely unexplored and certainly deserve attention.

This topic is also related to design of catalysts with noninnocent ligands. The recognition that "spectator" ligands can sometimes be active in catalysis [110] revealed interesting possibilities for future catalyst design. Catalysts in which an unreactive ligand is coupled to a reactive group would be much less susceptible to Schlenk equilibria and could especially in enantioselective catalysis be important.

In contrast to Al catalysis [111], the potential of redox-active noninnocent ligands has so far not been exploited in early main group metal catalysis. Ligands that can act as reversible electron reservoirs could significantly expand the toolbox of s-block metal catalysis bringing them further at par with transition metals. First, reversible redox reactions with Mg complexes have been reported [112], and there is also increasing interest in complexes with highly charged π-systems, which can act as electron supply [113].

Finally, given the importance of heterogeneous catalysis in the industry, support of catalysts on surfaces or synthesis of defined insoluble catalysts from molecular precursors, possibly with control over morphology and/or porosity, can expand the possibilities even further, thus creating continuously moving horizons.

List of Abbreviations

Ae	alkaline earth
AIM	atoms-in-molecules
N″	$N(SiMe_3)_2$
NPA	natural population analysis
Tf	triflate = $CF_3S(O)_2O$
THF	tetrahydrofuran
THP	tetrahydropyran

References

1 Frankland, E. (1849). *Ann. Chem. Pharm.* 71: 213–215.
2 For historical reviews see: (a)Seyferth, D. (2001). *Organometallics* 20: 2940–2955. (b) Seyferth, D. (2006). *Organometallics* 25: 2–24. (c) Seyferth, D. (2009). *Organometallics* 28: 2–33.

3 "In trockenem Zustand stellt das Lithiummethyl ein vollkommen farbloses mikrokrystallinisches Pulver dar. An die Luft gebracht, verbrennt es mit explosionsartiger Heftigkeit. Die auftretende Flamme besitzt die schöne Rotfärbung, welche fur die Lithiumflamme charakteristisch ist; da zahlreiche aus der roten Flamme fortgeschleuderte Funken gelbglühend sind, gewährt das Abbrennen von Lithiummethyl einen prächtigen Anblick." Schlenk, W. and Holtz, J. (1917). *Ber. Dtsch. Chem. Ger.* 50: 271.

4 Tidwell, T.T. (2001). *Angew. Chem. Int. Ed.* 40: 331–337.

5 Ziegler, K. and Colonius, H. (1930). *Liebigs Ann. Chem.* 479: 135–149.

6 Grignard, V. (1900). *C.R. Acad. Sci.* 130: 1322–1324.

7 Beckmann, E. (1905). *Ber. Dtsch. Chem. Ges.* 38: 904–906.

8 Gilman, H. and Schulze, F. (1926). *J. Am. Chem. Soc.* 48: 2463–2467.

9 Schlosser, M. (2002). *Organometallics in Synthesis: A Manual*, 2e. New York: Wiley.

10 (a) Brandsma, L. and Verkruijsse, H. (1987). *Preparative Polar Organometallic Chemistry 1*. Berlin: Springer-Verlag. (b) Brandsma, L. and Verkruijsse, H. (1990). *Preparative Polar Organometallic Chemistry 2*. Berlin: Springer-Verlag.

11 Smith, M.B. (2013). *March's Advanced Organic Chemistry*, 7e, 314. Hoboken, NJ: Wiley.

12 pK_a values of alkanes are difficult to estimate and different scales have been reported: (a)Cram, D.J. (1965). *Fundamentals of Carbanion Chemistry*. New York: W. A. Benjamin, Inc. (b) Dessy, R.E., Kitching, W., Psarras, T. et al. (1966). *J. Am. Chem. Soc.* 88: 460–467. (c) Robertson, P.J., Scurrell, M.S., and Kemball, C. (1975). *J. Chem. Soc., Faraday Trans. 1* 71: 903–912.

13 (a) Whisler, M.C., MacNeil, S., Snieckus, V., and Beak, P. (2004). *Angew. Chem. Int. Ed.* 43: 2206–2225. (b) Tilly, D., Magolan, J., and Mortier, J. (2012). *Chem. Eur. J.* 18: 3804–3820.

14 Farnham, W.B. and Calabrese, J.C. (1986). *J. Am. Chem. Soc.* 108: 2449–2451.

15 Fu, P.-F., Khan, M.A., and Nicholas, M. (1992). *J. Am. Chem. Soc.* 114: 6579–6580.

16 Lochmann, L. and Janata, M. (2014). *Cent. Eur. J. Chem.* 12: 537–548.

17 (a) Lochmann, L., Pospíšil, J., and Lim, D. (1966). *Tetrahedron Lett.*: 257–260. (b) Schlosser, M. (1967). *J. Organomet. Chem.* 8: 9–16.

18 Morton, A.A. and Chester, E.C. (1954). *J. Am. Chem. Soc.* 76: 4935–4938.

19 Mulvey, R.E., Mongin, F., Uchiyama, M., and Kondo, Y. (2007). *Angew. Chem. Int. Ed.* 46: 3802–3824.

20 Bickelhaupt, F. (1994). *J. Organomet. Chem.* 475: 1–14.

21 Naglav, D., Buchner, M.R., Bendt, G. et al. (2016). *Angew. Chem. Int. Ed.* 55: 10562–10576.

22 (a) Condorelli, G.G., Malandrino, G., and Fragalà, I.L. (2007). *Coord. Chem. Rev.* 251: 1931–1950. (b) Kim, S.B., Yang, C., Powers, T. et al. (2016). *Angew. Chem. Int. Ed.* 55: 10228–10233.

23 (a) Harder, S. (2010). *Chem. Rev.* 110: 3852–3876. (b) Barrett, A.G.M., Crimmin, M.R., Hill, M.S., and Procopiou, P.A. (2010). *Proc. R. Soc. Math. Phys. Eng. Sci.* 466: 927–963. (c) Westerhausen, M. (2009). *Z. Allg. Anorg. Chem.* 635: 13–32. (d) Hill, M.S., Liptrot, D.J., and Weetman, C. (2016).

Chem. Soc. Rev. 45: 972–988. (e) Sarazin, Y. and Carpentier, J.-F. (2016). *Chem. Rec.* 16: 2482–2505. (f) Crimmin, M.R. and Hill, M.S. (2013). *Alkaline-Earth Metal Compounds: Oddities and Applications*, vol. 45 (ed. S. Harder), 191–241. Heidelberg: Springer. (g) Rochat, R., Lopez, M.J., Tsurugi, H., and Mashima, K. (2016). *ChemCatChem* 8: 10–20.

24 (a) Westerhausen, M., Koch, A., Görls, H., and Krieck, S. (2017). *Chem. Eur. J.* 23: 1456–1483. (b) Westerhausen, M., Langer, J., Krieck, S. et al. (2013). *Alkaline-Earth Metal Compounds: Oddities and Applications*, vol. 45 (ed. S. Harder), 29–72. Heidelberg: Springer.

25 Schlenk, W. and Schlenk, W. Jr., (1929). *Ber. Dtsch. Chem. Ges.* 62B: 920–924.

26 Langer, J., Gärtner, M., Fischer, R. et al. (2007). *Inorg. Chem. Commun.* 10: 1001–1004.

27 Westerhausen, M. (1991). *Inorg. Chem.* 30: 96–101.

28 Brady, E.D., Hanusa, T.P., Pink, M., and Young, V.G. Jr., (2000). *Inorg. Chem.* 39: 6028–6037.

29 Johns, A.M., Chmely, S.C., and Hanusa, T.P. (2009). *Inorg. Chem.* 48: 1380–1384.

30 Harder, S., Feil, F., and Weeber, A. (2001). *Organometallics* 20: 1044–1046.

31 Feil, F., Müller, C., and Harder, S. (2003). *J. Organomet. Chem.* 683: 56–63.

32 Harder, S., Müller, S., and Hübner, E. (2004). *Organometallics* 23: 178–183.

33 Feil, F. and Harder, S. (2001). *Organometallics* 20: 4616–4622.

34 Weeber, A., Harder, S., and Brintzinger, H.-H. (2000). *Organometallics* 19: 1325–1332.

35 Izod, K. and Waddell, P.G. (2015). *Organometallics* 34: 2726–2730.

36 Jochmann, P., Dols, T.S., Spaniol, T.P. et al. (2009). *Angew. Chem. Int. Ed.* 48: 5715–5719.

37 Eaborn, C., Hawkes, S.A., Hitchcock, P.B., and Smith, J.D. (1997). *Chem. Commun.*: 1961–1962.

38 Cloke, F.G.N., Hitchcock, P.B., Lappert, M.F. et al. (1991). *J. Chem. Soc., Chem. Commun.*: 724–725.

39 Crimmin, M.R., Barrett, A.G.M., Hill, M.S. et al. (2008). *Chem. Eur. J.* 14: 11292–11295.

40 Feil, F. and Harder, S. (2000). *Organometallics* 19: 5010–5015.

41 Köhler, M., Koch, A., Görls, H., and Westerhausen, M. (2016). *Organometallics* 35: 242–248.

42 Koch, A., Wirgenings, M., Krieck, S. et al. (2017). *Organometallics* 36: 3981–3986.

43 Causero, A., Elsen, H., Pahl, J., and Harder, S. (2017). *Angew. Chem. Int. Ed.* 56: 6906–6910.

44 Causero, A., Ballmann, G., Pahl, J. et al. (2017). *Dalton Trans.* 46: 1822–1831.

45 Wilson, A.S.S., Hill, M.S., Mahon, M.F. et al. (2017). *Science* 358: 1168–1171.

46 Wolf, B.M., Stuhl, C., Maichle-Mössmer, C., and Anwander, R. (2018). *J. Am. Chem. Soc.* 140: 2373–2383.

47 Rösch, B., Gentner, T.X., Elsen, H. et al. (2019). *Angew. Chem. Int. Ed.* 58: 5396–5401.

48 Vaartstra, B.A., Huffmann, J.C., Streib, W.E., and Caulton, K.G. (1991). *Inorg. Chem.* 30: 121–125.

49 Deacon, G.B., Jaroschik, F., Junk, P.C., and Kelly, R.P. (2015). *Organometallics* 34: 2369–2377.

50 Takahashi, Y., O'Brien, A., Deacon, G.B. et al. (2017). *Inorg. Chem.* 56: 11480–11489.

51 de Bruin-Dickason, C.N., Deacon, G.B., Jones, C. et al. (2019). *Eur. J. Inorg. Chem.*: 1030–1038.

52 (a) Buchanan, W.D., Allis, D.G., and Ruhlandt-Senge, K. (2010). *Chem. Commun.* 46: 4449–4465. (b) Torvisco, A. and Ruhlandt-Senge, K. (2013). *Alkaline-Earth Metal Compounds: Oddities and Applications*, vol. 45 (ed. S. Harder), 1–28. Heidelberg: Springer.

53 Schleyer, P.v.R. and Lambert, C. (1994). *Angew. Chem. Int. Ed. Engl.* 33: 1129–1140.

54 Pauling, L. (1960). *The Nature of the Chemical Bond*. Ithaca, NY: Cornell University Press.

55 (a) McKeever, L.D., Waack, R., Doran, M.A., and Baker, E.B. (1968). *J. Am. Chem. Soc.* 90: 3244. (b) Brown, T.L., Seitz, L.M., and Kimura, B.Y. (1968). *J. Am. Chem. Soc.* 90: 3245. (c) McKeever, L.D., Waack, R., Doran, M.A., and Baker, E.B. (1969). *J. Am. Chem. Soc.* 91: 1057–1061.

56 Andrews, L. and Carver, T.G. (1968). *J. Chem. Phys.* 72: 1743–1747.

57 Streitwieser, A. Jr.,, Williams, J.E. Jr.,, Alexandratos, S., and McKelvey, J.M. (1976). *J. Am. Chem. Soc.* 98: 4778–4784.

58 Streitwieser, A. Jr., (1978). *J. Organomet. Chem.* 156: 1–3.

59 Graham, G.D., Marynick, D.S., and Lipscomb, W.N. (1980). *J. Am. Chem. Soc.* 102: 4572–4578.

60 Reed, A.E., Weinstock, R.B., and Weinhold, F. (1985). *J. Chem. Phys.* 83: 735–746.

61 Harder, S. (1990). A study on the structure and reactivity of aryllithium compounds with an α- or β-heteroatom. PhD thesis. University of Utrecht.

62 Smith, G.S., Johnson, Q.C., Smith, D.K. et al. (1988). *Solid State Commun.* 67: 491–494.

63 Wiesinger, M., Maitland, B., Färber, C. et al. (2017). *Angew. Chem. Int. Ed.* 56: 16654–16659.

64 (a) Westerhausen, M. and Schwarz, W. (1992). *Z. Anorg. Allg. Chem.* 609: 39–44. (b) Westerhausen, M. and Schwarz, W. (1991). *Z. Anorg. Allg. Chem.* 604: 127–140. (c) Westerhausen, M. and Schwarz, W. (1991). *Z. Anorg. Allg. Chem.* 606: 177–190.

65 Bock, H., Hauck, T., Näther, C. et al. (1995). *Angew. Chem. Int. Ed. Engl.* 34: 1353–1355.

66 Maitland, B., Wiesinger, M., Langer, J. et al. (2017). *Angew. Chem. Int. Ed.* 56: 11880–11884.

67 Rosca, S.-C., Dinoi, C., Caytan, E. et al. (2016). *Chem. Eur. J.* 22: 6505–6509.

68 Pahl, J., Brand, S., Elsen, H., and Harder, S. (2018). *Chem. Commun.* 54: 8685–8688.

69 Brookhart, M., Green, M.L.H., and Parkin, G. (2007). *Proc. Natl. Acad. Sci. U.S.A.* 104: 6908–6914.

70 Scherer, W., Sirsch, P., Grosche, M. et al. (2001). *Chem. Commun.*: 2072–2073.

71 Liu, B., Roisnel, T., Carpentier, J.-F., and Sarazin, Y. (2013). *Chem. Eur. J.* 19: 13445–13462.

72 Fischer, C.A., Rösch, A., Elsen, H. et al. (2019). *Dalton Trans.* 48: 6757–6766.

73 Günther, H. (1999). *J. Braz. Chem. Soc.* 10: 241–262.

74 Seebach, D., Hässig, R., and Gabriel, J. (1983). *Helv. Chim. Acta* 66: 308–337.

75 Günther, H., Moskau, D., Bast, P., and Schmalz, D. (1987). *Angew. Chem. Int. Ed. Engl.* 26: 1212–1220.

76 Reich, H.J. (2013). *Chem. Rev.* 113: 7130–7178.

77 (a) McGarrity, J.F., Ogle, C.A., Brich, Z., and Loosli, H.-R. (1985). *J. Am. Chem. Soc.* 107: 1810–1815. (b) Jones, A.C., Sanders, A.W., Bevan, M.J., and Reich, H.J. (2007). *J. Am. Chem. Soc.* 129: 3492–3493.

78 Bauer, W. and Seebach, D. (1984). *Helv. Chim. Acta* 67: 1972–1988.

79 (a) Neufeld, R. and Stalke, D. (2015). *Chem. Sci.* 6: 3354–3364. (b) Neufeld, R., Teuteberg, T.L., Herbst-Irmer, R. et al. (2016). *J. Am. Chem. Soc.* 138: 4796–4806.

80 Lincoln, S.F. (2005). *Helv. Chim. Acta* 88: 523–545.

81 Balasanthiran, V., Chisholm, M.H., Choojun, K. et al. (2016). *Polyhedron* 103: 235–240.

82 Tammiku-Taul, J., Burk, P., and Tuulmets, A. (2004). *J. Phys. Chem. A* 108: 133–139.

83 Peltzer, R.M., Eisenstein, O., Nova, A., and Cascella, M. (2017). *J. Phys. Chem. B* 121: 4226–4237.

84 Ruspic, C. and Harder, S. (2007). *Inorg. Chem.* 46: 10426–10433.

85 Gentner, T.X., Rösch, B., Thum, K. et al. (2019). *Organometallics* 38: 2485–2493.

86 Dye, J.L. (1984). *J. Phys. Chem.* 88: 3842–3846.

87 Stasch, A. and Jones, C. (2011). *Dalton Trans.* 40: 5659–5672.

88 (a) Jones, C. (2017). *Nat. Chem. Rev.* 1: 0059. (b) Green, S.P., Jones, C., and Stasch, A. (2007). *Science* 318: 1754–1757.

89 Krieck, S., Görls, H., Yu, L. et al. (2009). *J. Am. Chem. Soc.* 131: 2977–2985.

90 Bullock, R.M. (2004). *Chem. Eur. J.* 10: 2366.

91 Wiberg, N. (2007). *Lehrbuch der Anorganischen Chemie*, 102e. Berlin: de Gruyter.

92 (a) Begouin, J.-M. and Niggemann, M. (2013). *Chem. Eur. J.* 19: 8030–8041. (b) Hong, L., Sun, W., and Wang, R. (2016). *RSC Green Chem. Ser.* 38 (Sustainable Catalysis, Part 1): 49–88. (c) Tsubugo, T., Yamashita, Y., and Kobayashi, S. (2013). *Alkaline-Earth Metal Compounds: Oddities and Applications*, vol. 45 (ed. S. Harder), 243–270. Heidelberg: Springer. (d) Yamashita, Y., Tsubogo, T., and Kobayashi, S. (2012). *Chem. Sci.* 3: 967–975. (e) Pelissier, H. (2017). *Org. Biomol. Chem.* 15: 4750–4782.

93 Kaufmann, E., Schleyer, P.v.R., Houk, K.N., and Wu, Y.-D. (1985). *J. Am. Chem. Soc.* 107: 5560–5562.

94 Dang, T.T., Boeck, F., and Hintermann, L. (2011). *J. Org. Chem.* 76: 9353–9361.

95 (a) Horn, A.H.C. and Clark, T. (2003). *J. Am. Chem. Soc.* 125: 2809–2816. (b) Schürer, G. and Clark, T. (1998). *Chem. Commun.*: 257–258.

96 (a) Harder, S. (2012). *Chem. Commun.* 48: 11165–11177. (b) Fohlmeister, L. and Stasch, A. (2015). *Aust. J. Chem.* 68: 1190–1201. (c) Mukherjee, D., Schuhknecht, D., and Okuda, J. (2018). *Angew. Chem. Int. Ed.* 57: 9590–9602. (d) Mukherjee, D. and Okuda, J. (2018). *Angew. Chem. Int. Ed.* 57: 1458–1473.

97 (a) Banerjee, S., Yang, Y.-F., Jenkins, I.D. et al. (2017). *J. Am. Chem. Soc.* 139: 6880–6887. (b) Liu, W.-B., Schuman, D.P., Yang, Y.-F. et al. (2017). *J. Am. Chem. Soc.* 139: 6867–6879.

98 Crimmin, M.R., Barrett, A.G.M., Hill, M.S., and Procopiou, P.A. (2007). *Org. Lett.* 9: 331–333.

99 Yadav, S., Dixit, R., Bisai, M.K. et al. (2018). *Organometallics* 37: 4576–4584.

100 Yadav, S., Pahar, S., and Sen, S.S. (2017). *Chem. Commun.* 53: 4562–4564.

101 Intemann, J., Lutz, M., and Harder, S. (2014). *Organometallics* 33: 5722–5729.

102 Barrett, A.G.M., Crimmin, M.R., Hill, M.S. et al. (2009). *Chem. Commun.*: 2299–2301.

103 Schumann, H., Schutte, S., Kroth, H.-J., and Lentz, D. (2004). *Angew. Chem. Int. Ed.* 43: 6208–6211.

104 Freitag, B., Elsen, H., Pahl, J. et al. (2017). *Organometallics* 36: 1860–1866.

105 Penafiel, J., Maron, L., and Harder, S. (2015). *Angew. Chem. Int. Ed.* 54: 201–206.

106 (a) Pahl, J., Stennet, T., Volland, M. et al. (2019). *Chem. Eur. J.* 25: 2025–2034.

107 Yu, Y., Smith, J.M., Flaschenriem, C.J., and Holland, P.L. (2006). *Inorg. Chem.* 45: 5742–5751.

108 Brand, S., Elsen, H., Langer, J. et al. (2018). *Angew. Chem. Int. Ed.* 57: 14169–14173.

109 Hatano, M., Moriyama, K., Maki, T., and Ishihara, K. (2010). *Angew. Chem. Int. Ed.* 49: 3823–3826.

110 Freitag, B., Fischer, C.A., Penafiel, J. et al. (2017). *Dalton Trans.* 46: 11192–11200.

111 Berben, L.A. (2015). *Chem. Eur. J.* 21: 2734–2742.

112 Dange, D., Gair, A.R., Jones, D.D.L. et al. (2019). *Chem. Sci.* 10: 3208–3216.

113 Causero, A., Elsen, H., Ballmann, G. et al. (2017). *Chem. Commun.* 53: 10386–10389.